Recombination and synaptic adjustment in oocytes of mice heterozygous for a large paracentric inversion

**Anna A. Torgasheva · Nikolai B. Rubtsov ·
Pavel M. Borodin**

Abstract Homologous chromosome synapsis in inversion heterozygotes results in the formation of inversion loops. These loops might be transformed into straight, non-homologously paired bivalents via synaptic adjustment. Synaptic adjustment was discovered 30 years ago; however, its relationship with recombination has remained unclear. We analysed this relationship in female mouse embryos heterozygous for large paracentric inversion In(1)1Rk using immunolocalisation of the synaptonemal complex (SYCP3) and mature recombination nodules (MLH1) proteins. The frequency of cells containing bivalents with inversion loops decreased from 69 % to 28 % during pachytene. If an MLH1 focus was present in the non-homologously paired inverted region of the straight bivalent, it was always located in the middle of the inversion. Most of the small, incompletely adjusted loops contained MLH1 foci near the points at which pairing partners were switched. This observation indicates that the degree of synaptic adjustment depended on the crossover position. Complete synaptic adjustment was only possible if a crossover (CO) was located exactly in the middle of the inversion. If a CO was located at any other site, this interrupted synaptic adjustment and resulted in inversion loops of different sizes with an MLH1 focus at or near the edge of the remaining loop.

Keywords Meiosis · Recombination · Synapsis · Synaptic adjustment · Inversion · MLH1

Abbreviations

CO	Crossover
Cy3	Orange fluorescing cyanine
DAPI	4′-6-Diamidino-2-phenylindole
DSB	Double-strand break
DOP-PCR	Degenerate oligonucleotide-primed polymerase chain reaction
dpc	Days post-conception
FISH	Fluorescent in situ hybridization
FITC	Fluorescein isothiocyanate
MLH1	MutL Homolog 1
NCO	Non-crossover
SC	Synaptonemal complex
SYCP3	Synaptonemal complex protein 3
TAMRA	Carboxytetramethylrhodamine

Responsible Editor: Beth A. Sullivan.

A. A. Torgasheva · N. B. Rubtsov · P. M. Borodin (✉)
Siberian Department, Institute of Cytology
and Genetics, Russian Academy of Sciences,
Novosibirsk 630090, Russia
e-mail: borodin@bionet.nsc.ru

N. B. Rubtsov · P. M. Borodin
Department of Cytology and Genetics,
Novosibirsk State University,
Novosibirsk, Russia

Introduction

Synapsis and recombination are the key processes of meiosis. In mammals, these events are initiated at the very beginning of meiotic prophase (leptotene stage)

by the formation of the axial elements of the synaptonemal complex (SC) along the cores of two sister chromatids and the scheduled generation of the numerous double-strand DNA breaks (DSBs). The resulting single-stranded DNA ends bind to RAD51, invade homologous regions and form heteroduplexes (early recombination nodules). Later, at zygotene, homologous chromosomes align and pair with each other, forming bivalents that are connected by the central elements of the SC. Synapsis is usually completed at pachytene, when DSBs are repaired through either the crossover (CO) or non-crossover (NCO) pathways (Youds and Boulton 2011). The CO sites (late recombination nodules) can be identified in SC spreads by immunostaining with antibodies against MLH1, a mismatch repair protein (Anderson et al. 1999; Baker et al. 1996; Barlow and Hulten 1998). At diakinesis–metaphase I, the late recombination nodules mature into chiasmata that link homologous chromosomes and facilitate their correct segregation to opposite poles (Handel and Schimenti 2010).

Chromosomal heterozygosity complicates the process of chromosome pairing. In inversion heterozygotes, strictly homologous synapsis results in formation of the inversion loops (Anderson et al. 1988; Batanian and Hulten 1987; Chandley 1982; Koehler et al. 2004). However, homologous pairing of the inverted regions is not always possible due to topological restrictions or a lack of synaptic initiation sites within these regions. Thus, these regions often pair non-homologously, forming straight bivalents (Ashley et al. 1993, 1981; Bardhan and Sharma 2000; Chandley et al. 1987; Cheng et al. 1999; Gabriel-Robez et al. 1988; Greenbaum and Reed 1984; Saadallah and Hulten 1986). Such bivalents might also occur due to the transformation of a homologously paired loop configuration. This suggestion came from the observations of Moses et al. (1982), who examined the synaptic behaviour of two paracentric inversions in male mice. These authors found a gradual decrease in the frequency of bivalents containing inversion loops and the relative size of the loops from early to late pachytene. They referred to this phenomenon "synaptic adjustment". The synaptic adjustment of inversion loops has been well documented in humans (Gabriel-Robez et al. 1986; Guichaoua et al. 1986), laboratory mice (Borodin et al. 2005; Chandley 1982; Davisson et al. 1981; Tease and Fisher 1986), pigs (Massip et al. 2010), chickens

(Kaelbling and Fechheimer 1985) and *Neurospora crassa* (Bojko 1990). However, its relationship with recombination remained unclear.

In this study, we examined chromosome pairing and recombination in female mice heterozygous for the large paracentric inversion In(1)1Rk, the same inversion in which Moses et al. (1982) discovered the phenomenon of synaptic adjustment. Because we were working with females, we were able to assess the dynamics of the synaptic adjustment by comparing loop frequency and size on successive days of oocyte development. This approach is more reliable than the traditional method of pachytene sub-staging in males based on morphological criteria (Ashley et al. 2004). We used fluorescent in situ hybridization (FISH) with chromosome painting probe to identify chromosome 1 in SC spreads and to detect inversion borders. Using immunolocalisation of MLH1, we visualized COs at pachytene (that is, during the course of synaptic adjustment). The immunolocalisation of RAD51 in SC spreads allowed us to estimate the delay in DSB repair in non-homologously paired regions.

Materials and methods

Animals

Male and female mice homozygous for the paracentric inversion In(1)1Rk were a generous gift from Dr. T. Roderick (The Jackson Laboratory, Bar Harbor, ME, USA). The inversion was transferred to the genetic background of the C57BL/6J strain using a series of consecutive backcrosses. This strain is currently maintained at the Institute of Cytology and Genetics as homozygous stock C57Bl/6J-In(1)1Rk/Icg. Female embryos heterozygous for In(1)1Rk inversion were generated by crossing 3-month-old males of this stock to 3-month-old C57BL/6J females. C57BL/6J embryos homozygous for the standard chromosome 1 were used as control. The day the uterine plug was observed was considered day 0 of gestation.

The preparation of the hybridization probe

The hybridization probe for chromosome 1 was prepared by microdissection from bone marrow chromosome spreads of a feral mouse homozygous for In (1)1Icg that was captured in Novosibirsk. In(1)1Icg

is a complex rearrangement involving two insertions of the homogeneously stained regions Is(HSR;1C5)1Icg and Is(HSR;1D)2Icg, separated by an inverted euchromatic segment between the 1C5 and 1E4 bands (Agulnik et al. 1990; Borodin et al. 1990a, b). These insertions increased the length of chromosome 1 by 50 % and made it an easy target for microdissection. The probe Dist1 was prepared by microdissection of the distal part of the rearranged chromosome 1 (Fig. 1), followed by degenerate oligonucleotide-primed polymerase chain reaction (DOP-PCR). The DNA fragments were labelled with TAMRA-dUTP in 17 additional PCR cycles.

SC spreading, immunostaining, fluorescent in situ hybridization, microscopy and imaging

Pregnant mice from 16 to 18 days post-conception (dpc) were sacrificed by cervical dislocation after anaesthesia. Oocytes were collected from embryonic ovaries according to Speed and Chandley (1983). Chromosome spreads were prepared according to Peters et al. (1997). Immunostaining was performed as described by Anderson et al. (1999) using rabbit polyclonal anti-SYCP3 (1:500; Abcam), mouse monoclonal anti-MLH1 (1:50; Abcam) and rabbit polyclonal anti-RAD51 (1:200; Abcam) primary antibodies. The secondary antibodies used were Cy3-conjugated goat anti-rabbit (1:500; Jackson ImmunoResearch), fluorescein isothiocyanate (FITC)-conjugated goat anti-mouse (1:50;

Jackson ImmunoResearch) and FITC-conjugated goat anti-rabbit (1:200; Jackson ImmunoResearch). All antibodies were diluted in PBT (3 % bovine serum albumin and 0.05 % Tween 20 in phosphate-buffered saline). A solution of 10 % PBT was used to perform the blocking. Primary antibody incubations were performed overnight in a humid chamber at 37 °C, and secondary antibody incubations were performed for 1 h at 37 °C. Finally, slides were mounted in Vectashield with 4′-6-diamidino-2-phenylindole (DAPI; Vector Laboratories) to stain the DNA and reduce fluorescence fading.

The preparations were visualized with an Axioplan 2 microscope (Carl Zeiss) equipped with a CCD camera (CV M300, JAI), CHROMA filter sets and ISIS4 image-processing package (MetaSystems GmbH). MLH1 and RAD51 signals were scored only if they were observed on the SCs of completely paired bivalents. The location of each imaged immunolabelled spread was recorded so that it could be relocated on the slide after FISH.

After acquisition of the immunofluorescence signals, the oocyte preparations were subjected to FISH with the probe Dist1 according to a standard protocol. Dispersed repeats were suppressed with mouse Cot-1 DNA.

Measurements and statistical analyses

The centromeric ends of the SCs were identified as bright DAPI-positive clouds of AT-rich heterochromatin (Fig. 2a). Bivalent 1 and its inversion breakpoints were
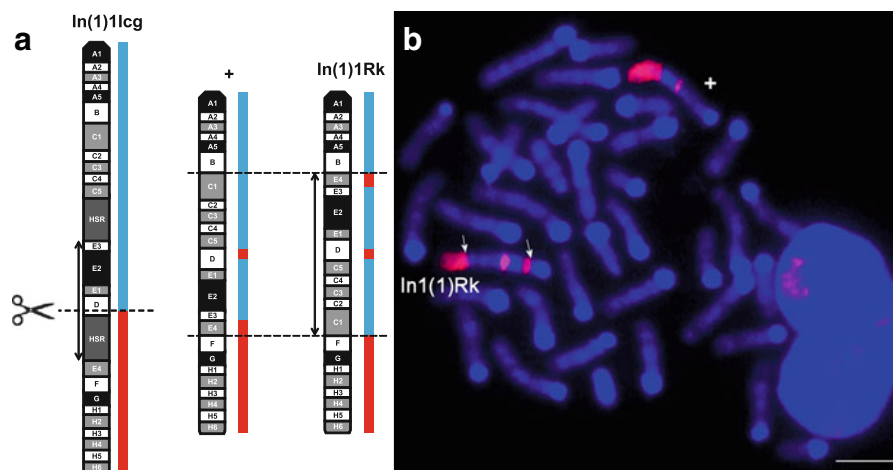

Fig. 1 Detection of mouse chromosome 1 and its inversion breakpoints with microdissected DNA probe Dist1. a A schematic representation of the In(1)1Icg chromosome, from which the probe was prepared, and the location of the probe on normal (+) and In(1)1Rk chromosomes. b FISH of the Dist1 probe to mitotic metaphase spreads from an In(1)1Rk/+ mouse. Red: Dist1 probe. Blue: DAPI. Arrows indicate the inversion breakpoints. Bar represents 5 μm
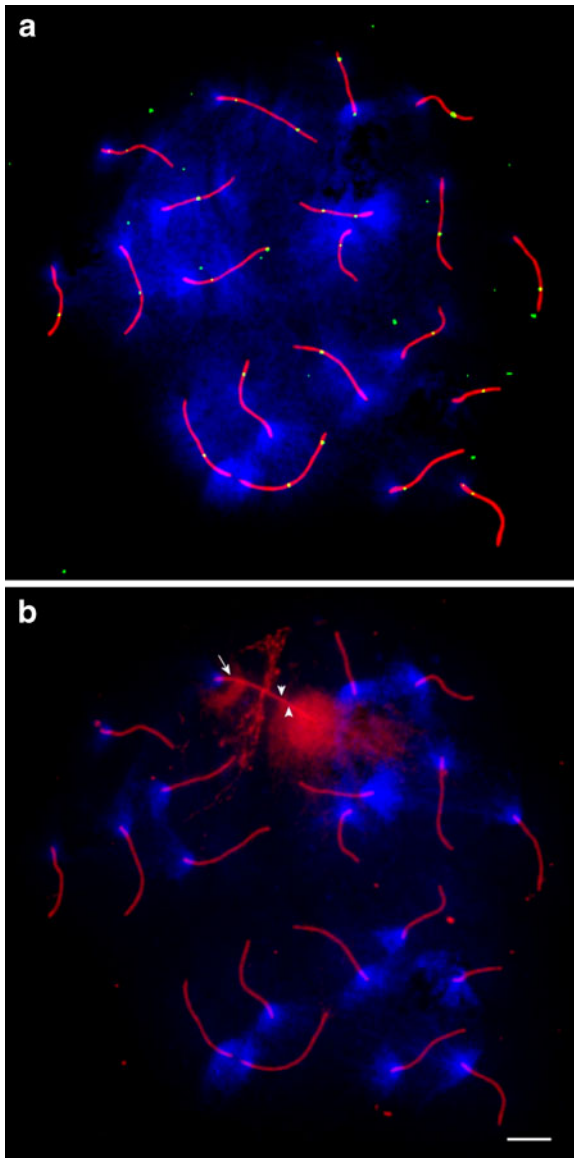
Fig. 2 A pachytene oocyte from a In1/+ mouse with a straight Chr 1 bivalent. **a** Immunostaining with antibodies to SYCP3 (*red*) and MLH1 (*green*) and counterstaining with DAPI (*blue*). **b** FISH with the Dist1 probe (*diffuse red*). The *arrow* indicates the proximal inversion breakpoint. *Arrowheads* indicate proximal borders of the distal signals from the normal homologue (*left*) and the In1 homologue (*right*). Note DAPI clouds around centromeres. *Bar* represents 5 μm

and (d) the distal inversion breakpoint. We also recorded the positions of the MLH1 foci relative to the centromere. These distances were then converted to fractions of the bivalent length. Figure 3 shows an example of these measurements. Based on these measurements, we estimated the relative lengths of the homologously paired proximal and distal non-inverted regions (from the proximal inversion breakpoint to the centromere and from the distal inversion breakpoint to the telomere), the homologously paired inverted region (between the loop edges) and the non-homologously synapsed or/and asynapsed parts of the inverted region.

Statistical analysis was conducted using the Statistica 6.0 software package (StatSoft, Tulsa, OK, USA).

Results

FISH with a microdissected probe visualizes the borders of the inversion

We tested the hybridization probe Dist1 in mitotic metaphase spreads prepared from the bone marrow of a In1/+ mouse (Fig. 1b). On the normal chromosome, this probe hybridized to two regions: the
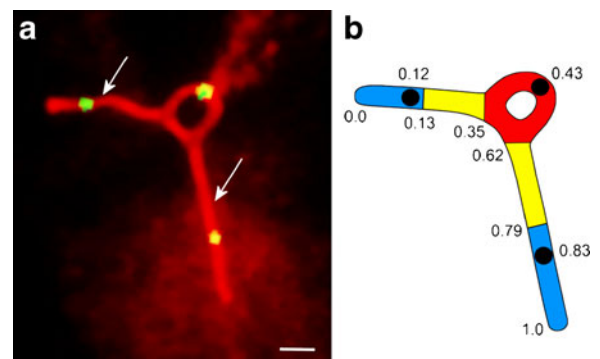

Fig. 3 Illustration of SC measurements. **a** Example of the SC of Chr 1 with an inversion loop, immunostained with antibodies to SYCP3 (*red*) and MLH1 (*green*). The *arrows* show the inversion breakpoints. *Bar* represents 1 μm. **b** A schematic representation of the SC, marked with the measurements. The relative positions of the MLH1 foci (*black dots*) are shown *above the schematic*. The relative positions of the proximal inversion breakpoint, proximal edge of the loop, distal edge of the loop and distal inversion breakpoint are shown *left to right below the schematic*. Homologously paired proximal and distal non-inverted regions are shown in *blue*, homologously paired inverted region is in *red* and non-homologously paired and asynapsed regions are in *yellow*

identified by the probe Dist1 (Fig. 2b). Using MicroMeasure3.3 (Reeves 2001), we measured the total length of the Chr 1 bivalent and the distance between its centromeric end and (a) the proximal inversion breakpoint, (b) the proximal edge of the synapsed part of the loop, (c) the distal edge of the synapsed part of the loop

proximal part of the D-band and the entire distal part of the chromosome, beginning from band E4.

On the inverted chromosome, we detected three signals: a proximal signal at band E4, marking the proximal inversion border; an interstitial signal within the inversion at a part of the D-band; and a distal signal hybridising from the F-band to the telomeric region, marking the distal inversion border (Fig. 1).

In the SC spreads of the Chr 1 bivalent in the inversion heterozygotes, the proximal edge of the proximal FISH signal served as an unequivocal mark of the proximal inversion breakpoint. The distal inversion breakpoint was more difficult to assign. The proximal edge of the signal from the DNA of the inverted homologue coincided with the inversion breakpoint, while the signal from the normal partner extended beyond the breakpoint to band E4, which was always paired non-homologously with band C1. However, in most spreads, it was possible to detect a difference between the signals and identify the distal breakpoint of the inversion (Fig. 2b).

The proximal breakpoint was located at an average relative distance (±SE) of 0.15±0.010 chromosome length from the centromere, while the distal point was located at 0.75±0.003 from the centromere. This is consistent with the relative position of the breakpoints observed in the mitotic metaphase chromosomes (Fig. 1).

The frequency of cells containing inversion loops decreases during meiotic progression

We observed two types of completely paired Chr 1 bivalents: those with inversion loops of various sizes (Fig. 4a–c) and the straight bivalents (Fig. 4d). Most straight bivalents were homologously paired in the proximal and distal collinear regions and non-homologously paired in the inversion region. We observed one straight bivalent in which both ends exhibited Dist1 signals. This indicates that the chromosomes were paired in an antiparallel orientation with the inverted region paired homologously and the non-inverted paired non-homologously (Fig. 4h). Most of the oocytes sampled from the inversion heterozygotes at 16–18 dpc contained a completely paired Chr 1 bivalent (Fig. 4a–d). We observed asynapsis in the pericentromeric (Fig. 4e) or inverted region (Fig. 4f) or both (Fig. 4g) in only 3 % of oocytes. Asynapsis in the distal non-inverted region was rare (<0.5 %). Bivalents with partial asynapsis (comprising about 9 % of the SC length) around the edges of the loops (Fig. 4b) were observed in 29 % of cells at 16 dpc, 5 % of cells at 17 dpc and 3 % of cells at 18 dpc.

The frequency of cells containing the loops decreased from 69 % to 28 % from 16 to 18 dpc (Table 1). Apparently, some loop-bearing bivalents underwent a synaptic adjustment and were transformed into the straight bivalents during pachytene. However, approximately one-third of oocytes contained straight Chr 1 bivalents even at 16 dpc, when most cells were at early pachytene. Such bivalents could have occurred due to synapsis extending from the edges of the chromosome into the inversion region.

The relative size of the inversion loops does not change during pachytene

The relative size of the synapsed part of the inversion loop varied in a wide range (Fig. 5). The largest loops involved up to 58 % of the bivalent length; the smallest comprised approximately 2–3 %, appearing as knots. Even the largest loops never involved the entire inverted region. Both loop borders were always located within the inverted region, often far from the inversion borders. Thus, a large part of the inversion was non-homologously paired.

We did not observe significant difference in average loop size between cells sampled at different dpc ($F=1.8$; $p=0.2$; Table 1).

The number and distribution of MLH1 foci in the Chr 1 bivalent depends on the synaptic configuration

The number of MLH1 foci in the Chr 1 bivalent tended to be higher at 17 dpc than at 16 and 18 dpc (Table 1). However, these differences were not significant ($F_{2,961}=2.7$; $p=0.06$); therefore, we pooled these data. Table 2 shows the mean number of MLH1 foci in normal homozygotes and in different synaptic configurations of the Chr 1 bivalent in the inversion heterozygotes.

The normal homozygotes displayed a relatively even distribution of the foci along the bivalent, with three slight elevations in the proximal, medial and distal regions (Fig. 6). In bivalents with a single MLH1 focus, the focus was usually located in the medial region. In bivalents with two MLH1 foci, the foci were typically located in the proximal and distal regions. Bivalents containing three MLH1 foci were very rare (0.7 %).
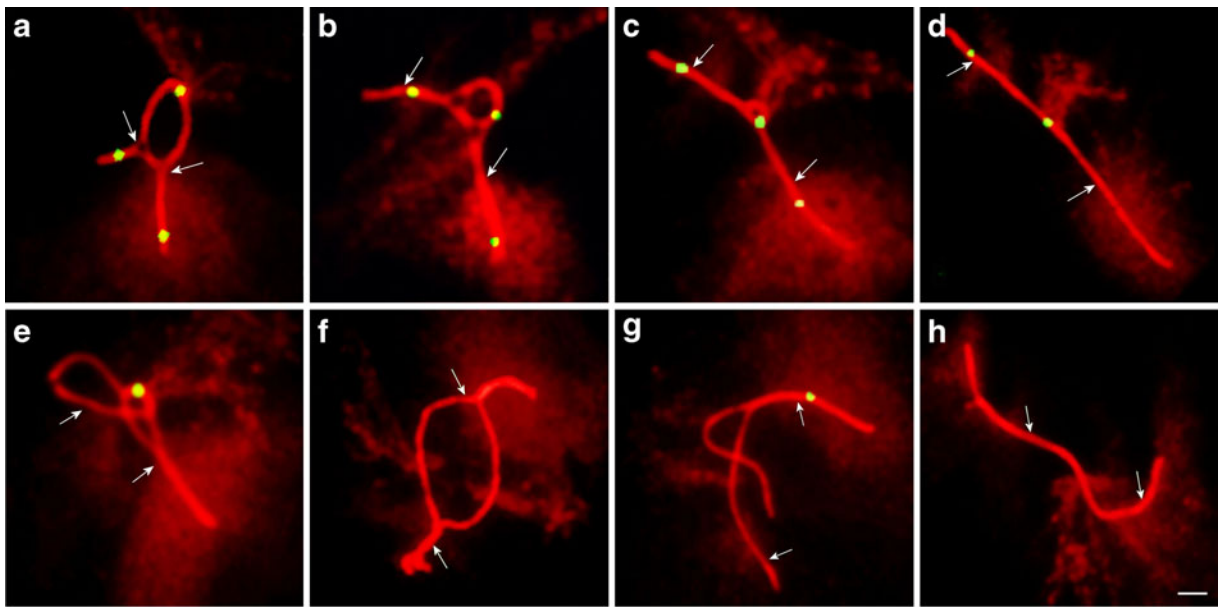
Fig. 4 Synaptic configurations of the Chr 1 bivalent in In1/+ mice. Combined images of the cells after sequential immunostaining with antibodies to SYCP3 (*red*) and MLH1 (*green*) and FISH with the Dist1 probe (*diffuse red*). The *arrows* indicate the inversion breakpoints. **a–c** Inversion loops of different sizes. **d** Straight bivalent. **e** Asynapsed pericentromeric region. **f** Asynapsed inverted region. **g** Asynapsed pericentromeric and inverted regions. **h** Anti-parallel synapsis (both chromosome ends show Dist1 signals). *Bar* represents 1 μm

The number of MLH1 foci in the loop-bearing bivalents was 37 % higher than that in the normal homozygotes (Mann–Whitney $Z=8.88$, $p<0.001$; Table 2). This phenomenon is likely due to an increase in the frequency of the bivalents containing three MLH1 foci at the expense of those containing one focus.

The distribution of MLH1 foci was also altered. Bivalents with loops displayed a more prominent pattern: there were conspicuous peaks in the proximal and distal regions. Within the inverted region, there was a steeper peak in the middle of the inversion and a lack of foci around its borders (Fig. 6).

We often observed MLH1 foci at or very near the loop ends (e.g. Fig. 4c). To quantify this phenomenon, we analysed the relative distance between the MLH1 focus located inside the loop and the nearest border of the loop (Fig. 7). The resulting histogram had one clear peak located near the end of the loop. The Kolmogorov–Smirnov test demonstrated a significant difference between the observed and expected uniform distribution ($D=0.23$, $p<0.001$).

As mentioned above, most straight bivalents apparently occurred due to heterosynapsis in the inverted region. Because of the lack of homology in the

Table 1 Synaptic characteristics and MLH1 focus number of the Chr 1 bivalents in the oocytes of normal homozygotes (+/+) and inversion heterozygotes (In1/+) sampled at different days post-conception

Karyotype	dpc	N cells	Frequency of cells containing the loops	Relative size of the synapsed part of the loop[a]		SC length, μm		MLH1 focus number	
				Mean	SE	Mean	SE	Mean	SE
+/+	18	225				12.00	0.09	1.64	0.03
In1/+	16	91	0.69	0.28	0.001	15.06	0.19	1.91	0.08
In1/+	17	459	0.38	0.24	0.009	13.81	0.11	2.02	0.03
In1/+	18	414	0.28	0.25	0.012	13.02	0.01	1.92	0.03

[a] Ratio of the loop length to the total SC length

Fig. 5 Horizontal histogram of between-cell variation in MLH1 foci positions (*black dots*), relatively lengths of homologously paired non-inverted regions from the centromere to the proximal inversion breakpoint and from the distal inversion breakpoint to the telomere (*blue*), homologously paired inverted region between the loop edges (*red*) and non-homologously synapsed and/or asynapsed parts of the inverted region (*yellow*). The colour code is the same as that in Fig. 3. The cells are sorted for dpc and for loop size in increasing order within each dpc sample
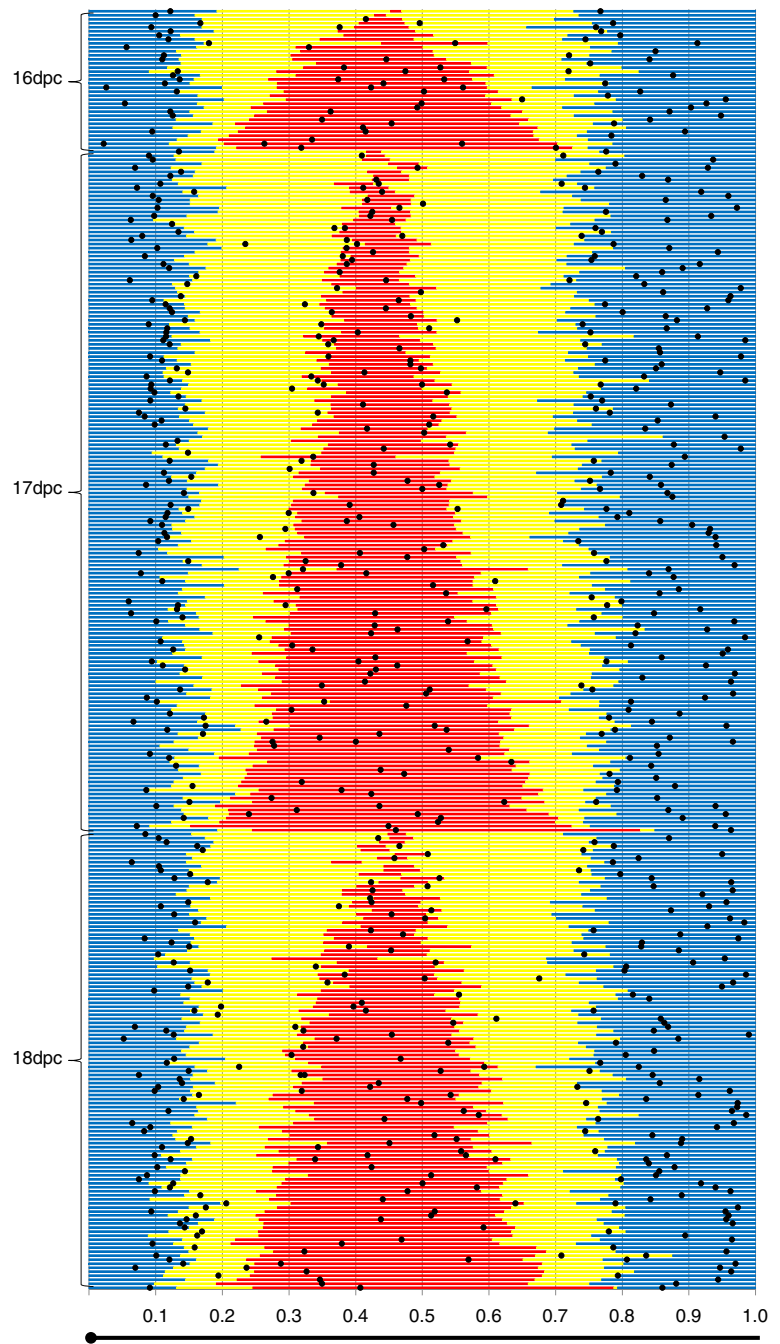
heterosynapsed region, crossing over and MLH1 foci would not be expected within the inversion. Three quarters of the straight bivalents observed at pachytene had no MLH1 foci inside the inversion, although the total number of foci was almost the same as that in the normal homozygotes. The lack of foci in the medial 60 % of the bivalent length was compensated by an increase in the number of MLH1 foci at its proximal and distal ends (Table 2).

The remaining one quarter of the straight bivalents did contain MLH1 foci in the inverted region (Fig. 4d). Average number of MLH1 foci at these bivalents was higher than in normal homozygotes and in the loop-bearing bivalents ($Z=9.05$, $p<0.001$; and 2.44,

$p<0.05$; Table 2). Remarkably, most of these MLH1 foci were located in the centre of the inversion (Fig. 6).

Chr 1 bivalent in inversion heterozygotes is excessively labelled by RAD51 at pachytene

As mentioned above, at 18 dpc (late pachytene), most oocytes contained a Chr 1 bivalent with the inverted region paired non-homologously (entirely in straight bivalents or partially in bivalents with loops). To assess the influence of non-homologous pairing on DSB repair, we estimated density of RAD51 foci (RAD51/SC length) of the Chr 1 bivalent and other bivalents in the inversion heterozygotes and controls (Table 3).

The loop and straight Chr 1 bivalents in the heterozygotes had a two-fold higher density of RAD51 than other bivalents ($Z=4.29$ and 6.05 correspondingly, $p<0.0001$) and normal Chr 1 bivalents ($Z=3.46$ and 4.90, $p<0.001$). In controls, Chr 1 bivalent and other bivalents had the same RAD51/SC ratio ($Z=1.16$, $p=0.25$).

Discussion

Synaptic adjustment depends on CO position

The formation of the inversion loop requires synapsis initiation at at least three sites: one within the inverted region and two outside. The paracentric inversion In (1)1Rk analysed here involves more than half of the chromosome length. The large size and central location of this inversion facilitate the loop formation in the heterozygotes. We observed a recombination peak in the middle of the inverted region in both the normal homozygotes and the inversion heterozygotes (Fig. 6). The high recombination frequency indicates a high probability of primary homolog association within the inversion, which triggers synapsis and loop formation.

Nevertheless, even at 16 dpc, when most cells were at the early pachytene stage, 31 % of bivalents were straight, with a non-homologously paired inversion region. Apparently, the earlier co-orientation of the flanking regions, facilitated by telomere clustering at leptotene (Scherthan 2007), suppressed the homologous alignment of the interstitial inverted region.

All loops were smaller than expected (Fig. 5), indicating that the "zipping up" of the SC proceeds from the flanking region to the inversion, rather than the other way around.

The frequency of loops decreased as pachytene progressed (Table 1). However, we did not observe a gradual decrease in the loop size. Similar results were obtained in male mice heterozygous for the same inversion In(1)1Rk (Anderson and Reeves 1998). Apparently, synaptic adjustment occurs very rapidly.

The most interesting finding in our study is that the size to which the loop can be adjusted depends on the position of the CO within the loop.

Moses et al. (1982) suggested that synaptic adjustment in inversion heterozygotes may suppress recombination within the inversions. They found that the COs inside the inversions (as measured by anaphase bridges) were half as frequent as expected. Moses et al. realized that once established, COs should pose topological restrictions to synaptic adjustment. However, these authors believed that synapsis preceded recombination. They considered synaptic adjustment as a gradual desynapsis of the inversion loop with subsequent resynapsis initiating from both ends of the loop. They proposed that the regions closer to the ends would have to be adjusted first and subsequently become unavailable for recombination. In this model, the mid-inversion loop region would remain homosynapsed for the longest

Table 2 Number of MLH1 foci on the Chr 1 bivalents in the oocytes of the normal homozygotes (+/+) and inversion heterozygotes (In1/+)

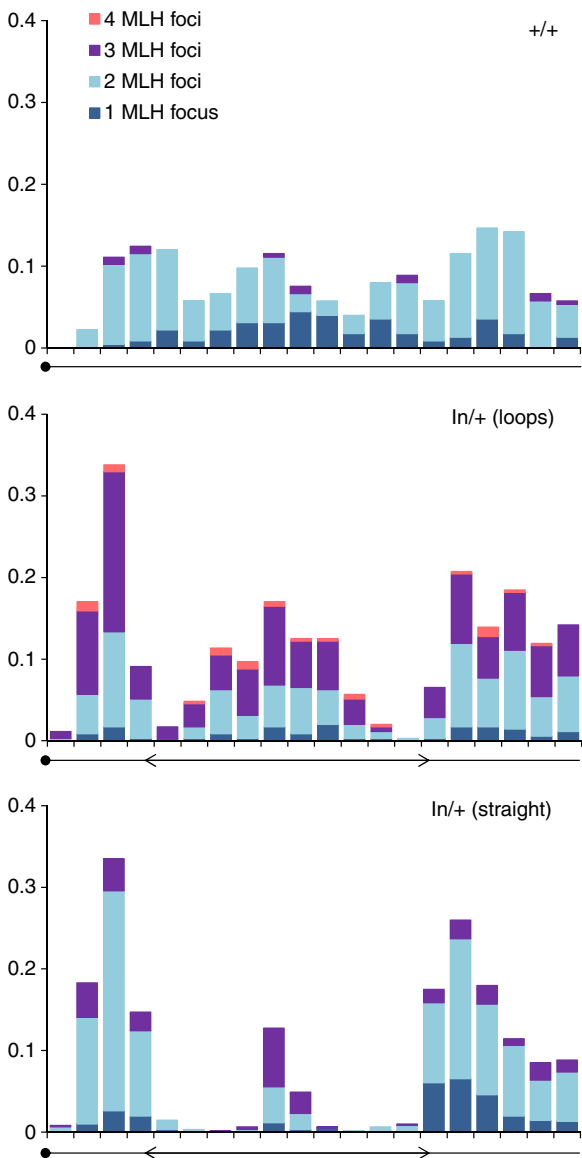| Karyotype	Configuration	N (SCs)	N (frequency) of cells containing				Mean	SE
			1 focus	2 foci	3 foci	4 foci		
+/+		225	84 (0.37)	137 (0.61)	4 (0.02)	0 (0)	1.64	0.03
In1/+	Loop	352	58 (0.16)	157 (0.45)	130 (0.37)	7 (0.02)	2.24	0.04
In1/+	Straight with MLH1 in the inversion	120	12 (0.10)	44 (0.37)	64 (0.53)	0 (0)	2.43	0.06
In1/+	Straight without MLH1 in the inversion	489	172 (0.35)	317 (0.65)	0 (0)	0 (0)	1.65	0.02

Fig. 6 Distribution of MLH1 foci along the Chr 1 bivalents in the oocytes of +/+ and In1/+ mice. The x-axis shows the position of the MLH1 foci; the marks are separated by intervals of 5 % of the chromosome length. *Stacked columns* show the frequency for the bivalents containing MLH1 foci in each interval. *Circles* indicate centromeres. *Arrows* indicate the approximate locations of the inversion breakpoints
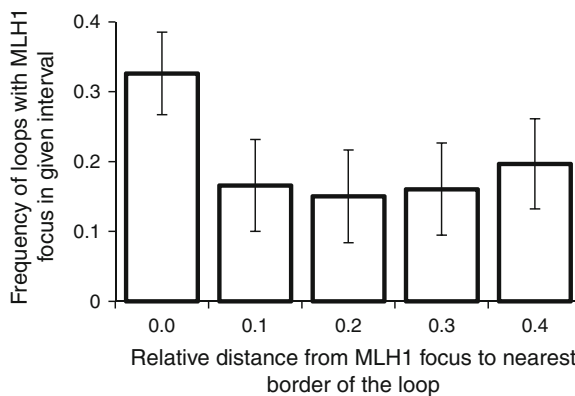

Fig. 7 The distribution of distances between MLH1 foci located within the inversion and the loop borders. The x-axis indicates the relative (fraction of the loop length) distance between each MLH1 focus and the nearest border of the loop. *Each column* represents the frequency of loops with an MLH1 focus within the given interval

period and therefore show the least reduction of CO frequency.

Now, it is known that stable recombination intermediates are formed before complete synapsis (Handel and Schimenti 2010). Therefore, synaptic adjustment cannot affect CO frequency. Conversely, CO position should affect the degree of the synaptic adjustment.

Complete synaptic adjustment (i.e. the transformation of loops into straight bivalents) may only be possible if a CO is located in the middle of the inversion. If a CO is located at any other place, it should interrupt synaptic adjustment and result in inversion loops of different sizes with an MLH1 focus at or near the edge of the remaining inversion loop.

Our results are consistent with these predictions. First, the MLH1 foci inside the inverted region of the straight bivalents were located mostly in the middle of the inversion. We also observed straight bivalents without MLH1 foci inside the inversions. These bivalents might result from immediate non-homologous synapsis at early pachytene or complete, unimpeded synaptic adjustment of the loops with no CO inside. Furthermore, we found that the distribution of the MLH1 foci inside the

Table 3 RAD51 focus density (number of foci per micrometre SC) in the pachytene oocytes of normal homozygotes (+/+) and inversion heterozygotes (In1/+)

Karyotype	Configuration	N cells	RAD51 density in the Chr 1 bivalent		RAD51 density in all other bivalents	
			Mean	SE	Mean	SE
+/+		90	0.14	0.01	0.15	0.09
In1/+	Loop	90	0.25	0.02	0.13	0.01
In1/+	Straight	100	0.28	0.02	0.12	0.01

incompletely adjusted loops was skewed toward the sites of pairing partner switching. This distribution could occur due to an accumulation of the loops in which adjustment had stopped at eccentrically located CO.

DSB repair is delayed in the inversion heterozygotes

Complete or partial non-homologous synapsis of the inverted region should affect the dynamics of DSB repair in the Chr 1 bivalent. In mice and yeast, most DSBs are repaired via inter-homolog recombination (Li et al. 2011; Schwacha and Kleckner 1997). Only a small fraction of DSBs are repaired using the sister chromatid as a template. Apparently, a kinetic difference in the speed of these processes leads to a preferential use of inter-homolog recombination over inter-sister recombination. In the local absence of donor sequences on the homolog, DSBs can be effectively repaired via inter-sister recombination, but this process tends to be slower (Goldfarb and Lichten 2010). In male mammals, DSBs remain unrepaired at the unsynapsed region of X chromosome until late pachytene/early diplotene; heavy RAD51 labelling is usually observed in this region, while most autosomes no longer exhibit RAD51 foci during this stage (Barlow et al. 1997; Moens et al. 1997).

Here, we demonstrated that the Chr 1 bivalents in inversion heterozygotes contained more RAD51 foci at late pachytene than normal Chr 1 bivalents or other bivalents. This indicates a delay in DSB repair in the inverted region. Plug et al. (1998) also observed an excess of RAD51 foci in asynapsed and heterosynapsed regions of double translocation heterozygotes of the chromosomes 1 and 13 in male mice. The delayed repair of DBSs in the heterozygotes for chromosome rearrangements may trigger apoptosis and reduce the fertility of the carriers (Burgoyne et al. 2009).

Inversion heterozygotes exhibit low crossover interference

Although a large segment of the Chr 1 bivalent was non-homologously paired in the inversion heterozygotes, these bivalents had higher numbers of COs than Chr 1 bivalent in normal homozygotes (Table 2). A similar increase in recombination frequency was observed in heterozygotes for the inversion In2(2)H that has a comparable location, absolute and relative size, and proportion of chromosome length occupied

(Koehler et al. 2004). The distribution of COs along the bivalent was also altered in the same way in both inversions. Heterozygotes for In1(1)Rk showed an unusual recombination peak near the centromere (Fig. 6). Similarly, the CO distribution in In2(2)H heterozygotes was shifted toward the proximal half of the SC (Koehler et al. 2004).

Observed increase in CO frequency and change in CO distribution were apparently determined by weaker interference between COs. Usually, the presence of one CO in a region decreases the probability that another CO will occur nearby (Berchowitz and Copenhaver 2010). However, our data indicate that COs separated by the point of pairing partner switching showed reduced interference or no interference at all.

The decreased interference in the inversion heterozygotes can be interpreted within the framework of "mechanical stress" model (Kleckner et al. 2004). This model addresses a physical system in which any changes in stress propagate in both directions from the starting point. As applied to meiotic chromosomes, the model suggests that primary CO site relieves the mechanical stress that spreads along the bivalent and prevents the appearance of secondary COs within a certain distance.

We suggest that changes in the spatial organization of bivalent (such as formation of inversion loops) impede the propagation of this "signal". In particular, the point of pairing partner changing could act as a barrier for CO interference. Non-homologous pairing of the inverted region and possible synaptic delay may also affect the rate of the transfer of any mechanical signal. As a result, the interference machinery acts independently within the regions separated by the points of pairing partner switching.

References

Agulnik SI, Borodin PM, Gorlov IP et al (1990) The origin of a double insertion of homogeneously staining regions in the house mouse (*Mus musculus musculus*). Heredity 65:265–267

Anderson LK, Reeves A (1998) Re-examining a mouse paracentric inversion heterozygote. The Society for Experimental Biology, Annual Meeting, 23–27 March, York, England, pp 55–56

Anderson LK, Stack SM, Sherman JD (1988) Spreading synaptonemal complexes from Zea mays. I. No synaptic adjustment of inversion loops during pachytene. Chromosoma 96(4):295–305

Anderson LK, Reeves A, Webb LM, Ashley T (1999) Distribution of crossing over on mouse synaptonemal complexes using immunofluorescent localization of MLH1 protein. Genetics 151(4):1569–1579

Ashley T, Moses MJ, Solari AJ (1981) Fine structure and behaviour of a pericentric inversion in the sand rat, Psammomys obesus. J Cell Sci 50:105–119

Ashley T, Cacheiro NL, Russell LB, Ward DC (1993) Molecular characterization of a pericentric inversion in mouse chromosome 8 implicates telomeres as promoters of meiotic recombination. Chromosoma 102(2):112–120

Ashley T, Gaeth AP, Creemers LB et al (2004) Correlation of meiotic events in testis sections and microspreads of mouse spermatocytes relative to the mid-pachytene checkpoint. Chromosoma 113(3):126–136

Baker SM, Plug AW, Prolla TA et al (1996) Involvement of mouse Mlh1 in DNA mismatch repair and meiotic crossing over. Nat Genet 13(3):336–342

Bardhan A, Sharma T (2000) Sequential meiotic prophase development in the pubertal Indian pygmy field mouse: synaptic progression of the XY chromosomes, autosomal heterochromatin, and pericentric inversions. Genome 43 (1):172–180

Barlow AL, Hulten MA (1998) Crossing over analysis at pachytene in man. Eur J Hum Genet 6(4):350–358

Barlow AL, Benson FE, West SC, Hulten MA (1997) Distribution of the Rad51 recombinase in human and mouse spermatocytes. EMBO J 16(17):5207–5215

Batanian J, Hulten MA (1987) Electron microscopic investigations of synaptonemal complexes in an infertile human male carrier of a pericentric inversion inv(1)(p32q42). Regular loop formation but defective synapsis including a possible interchromosomal effect. Hum Genet 76(1):81–89

Berchowitz LE, Copenhaver GP (2010) Genetic interference: don't stand so close to me. Curr Genomics 11(2):91–102

Bojko M (1990) Synaptic adjustment of inversion loops in Neurospora crassa. Genetics 124(3):593–598

Borodin PM, Gorlov IP, Ladygina T (1990a) Double insertion of homogeneously staining regions in chromosome 1 of wild Mus musculus musculus: effects on chromosome pairing and recombination. J Hered 81(2):91–95

Borodin PM, Gorlov IP, Ladygina T (1990b) Synapsis in single and double heterozygotes for partially overlapping inversions in chromosome 1 of the house mouse. Chromosoma 99(5):365–370

Borodin PM, Ladygina TY, Rodionova MI et al (2005) Genetic control of chromosome synapsis in mice heterozygous for a paracentric inversion. Russ J Genet 41(6):602–607

Burgoyne PS, Mahadevaiah SK, Turner JM (2009) The consequences of asynapsis for mammalian meiosis. Nat Rev Genet 10(3):207–216

Chandley AC (1982) A pachytene analysis of two male-fertile paracentric inversions in chromosome 1 of the mouse and in the male-sterile double heterozygote. Chromosoma 85 (1):127–135

Chandley AC, McBeath S, Speed RM et al (1987) Pericentric inversion in human chromosome 1 and the risk for male sterility. J Med Genet 24(6):325–334

Cheng EY, Chen YJ, Disteche CM, Gartler SM (1999) Analysis of a paracentric inversion in human oocytes: nonhomologous pairing in pachytene. Hum Genet 105(3):191–196

Davisson MT, Poorman PA, Roderick TH, Moses MJ (1981) A pericentric inversion in the mouse. Cytogenet Cell Genet 30(2):70–76

Gabriel-Robez O, Ratomponirina C, Rumpler Y et al (1986) Synapsis and synaptic adjustment in an infertile human male heterozygous for a pericentric inversion in chromosome 1. Hum Genet 72(2):148–152

Gabriel-Robez O, Ratomponirina C, Croquette M et al (1988) Synaptonemal complexes in a subfertile man with a pericentric inversion in chromosome 21. Heterosynapsis without previous homosynapsis. Cytogenet Cell Genet 48 (2):84–87

Goldfarb T, Lichten M (2010) Frequent and efficient use of the sister chromatid for DNA double-strand break repair during budding yeast meiosis. PLoS Biol 8(10):e1000520

Greenbaum IF, Reed MJ (1984) Evidence for heterosynaptic pairing of the inverted segment in pericentric inversion heterozygotes of the deer mouse (Peromyscus maniculatus). Cytogenet Cell Genet 38(2):106–111

Guichaoua MR, Delafontaine D, Taurelle R et al (1986) Loop formation and synaptic adjustment in a human male heterozygous for two pericentric inversions. Chromosoma 93 (4):313–320

Handel MA, Schimenti JC (2010) Genetics of mammalian meiosis: regulation, dynamics and impact on fertility. Nat Rev Genet 11(2):124–136

Kaelbling M, Fechheimer NS (1985) Synaptonemal complex analysis of a pericentric inversion in chromosome 2 of domestic fowl, Gallus domesticus. Cytogenet Cell Genet 39(2):82–86

Kleckner N, Zickler D, Jones GH et al (2004) A mechanical basis for chromosome function. Proc Natl Acad Sci U S A 101(34):12592–12597

Koehler KE, Millie EA, Cherry JP et al (2004) Meiotic exchange and segregation in female mice heterozygous for paracentric inversions. Genetics 166(3):1199–1214

Li XC, Bolcun-Filas E, Schimenti JC (2011) Genetic evidence that synaptonemal complex axial elements govern recombination pathway choice in mice. Genetics 189(1):71–82

Massip K, Yerle M, Billon Y et al (2010) Studies of male and female meiosis in inv(4)(p1.4;q2.3) pig carriers. Chromosome Res 18(8):925–938

Moens PB, Chen DJ, Shen Z et al (1997) Rad51 immunocytology in rat and mouse spermatocytes and oocytes. Chromosoma 106(4):207–215

Moses MJ, Poorman PA, Roderick TH, Davisson MT (1982) Synaptonemal complex analysis of mouse chromosomal rearrangements. IV. Synapsis and synaptic adjustment in two paracentric inversions. Chromosoma 84:457–474.

Peters AH, Plug AW, van Vugt MJ, de Boer P (1997) A drying-down technique for the spreading of mammalian meiocytes from the male and female germline. Chromosome Res 5 (1):66–68

Plug AW, Peters AH, Keegan KS et al (1998) Changes in protein composition of meiotic nodules during mammalian meiosis. J Cell Sci 111:413–423

Reeves A (2001) MicroMeasure: a new computer program for the collection and analysis of cytogenetic data. Genome 44 (3):439–443

Saadallah N, Hulten M (1986) EM investigations of surface spread synaptonemal complexes in a human male carrier of a pericentric inversion inv(13)(p12q14): the role of heterosynapsis for spermatocyte survival. Ann Hum Genet 50:369–383

Scherthan H (2007) Telomere attachment and clustering during meiosis. Cell Mol Life Sci 64(2):117–124

Schwacha A, Kleckner N (1997) Interhomolog bias during meiotic recombination: meiotic functions promote a highly differentiated interhomolog-only pathway. Cell 90 (6):1123–1135

Speed RM, Chandley AC (1983) Meiosis in the foetal mouse ovary. II. Oocyte development and age-related aneuploidy. Does a production line exist. Chromosoma 88(3):184–189

Tease C, Fisher G (1986) Further examination of the production-line hypothesis in mouse foetal oocytes. I. Inversion heterozygotes. Chromosoma 93(5):447–452

Youds JL, Boulton SJ (2011) The choice in meiosis—defining the factors that influence crossover or non-crossover formation. J Cell Sci 124:501–513